

Supporting Information

Structure and regulatory interactions of the cytoplasmic terminal domains of serotonin transporter

Cristina Fenollar-Ferrer, Thomas Stockner, Thomas C. Schwarz, Aritra Pal, Jelena Gotovina, Tina Hofmaier, Kumaresan Jayaraman, Suraj Adhikary, Oliver Kudlacek, Ahmad Reza Mehdipour, Sotiria Tavoulari, Gary Rudnick, Satinder K. Singh, Robert Konrat, Harald H. Sitte, Lucy R. Forrest



Figure S1. Sequence alignment of dDAT and SERT. Pairwise alignment of dDAT (PDB entry 4M48) and SERT used for constructing the model of the transmembrane regions of outward-facing SERT. The transmembrane segments in the dDAT structure are outlined with black boxes, as is the missing segment in extracellular loop 2 (EL2).

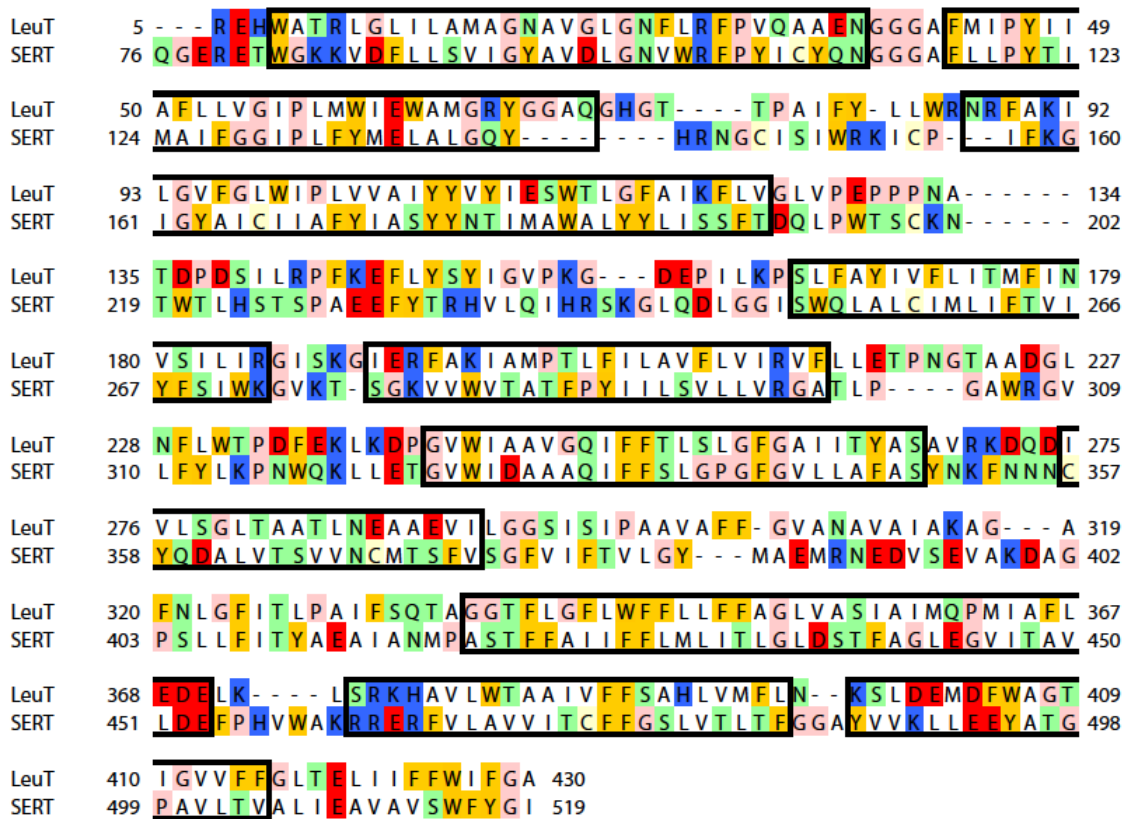


Figure S2. *Sequence alignment of LeuT and SERT.* Pairwise alignment of LeuT mutant crystallized in an inward-facing conformation (PDB entry 3TT3) and SERT, for residues corresponding to TM1-10 of LeuT. The transmembrane segments in the LeuT structure are outlined with black boxes. Residues in TM1a (5-REHWAT-10) not present in this structure were instead modeled on a structure of LeuT in an outward-facing conformation (PDB entry 2A65) – see Experimental Procedures section for details.

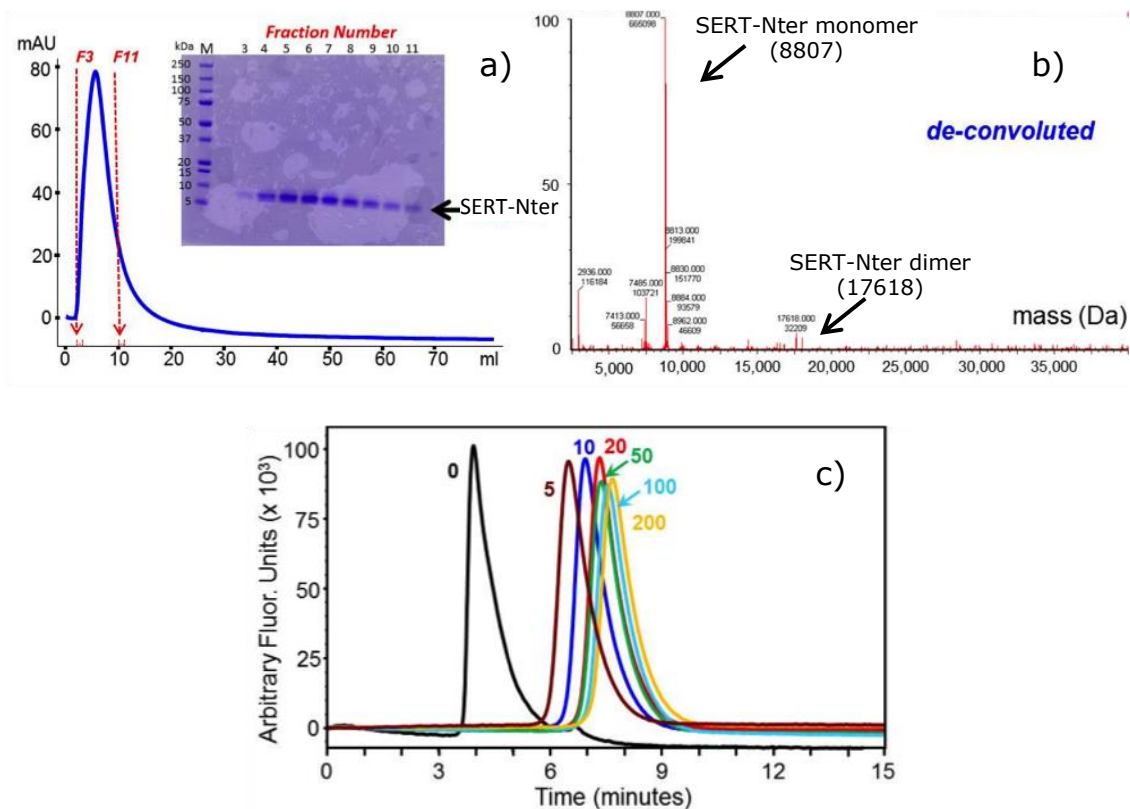


Figure S3: Purification, mass spectrum and FSEC of SERT-Nter peptide. (a) SDS-PAGE of SERT-Nter flow-through fractions from final HisPrep chromatographic run. (b) Electrospray ionization mass spectrometry (ESI-MS) of SERT-Nter. (c) FSEC runs (monitoring tryptophan fluorescence) of SERT-Nter in 20 mM phosphate (pH 7.4) and the indicated concentrations of NaCl. Initial CD experiments on SERT-Nter were conducted with 25 μ M protein in buffer B (20 mM Tris [pH 8], 200 mM NaCl, 5 mM β -ME) at 20°C on an Applied Photophysics Chirascan Circular Dichroism Spectrophotometer using a 1 mm quartz cuvette (Hellma Analytics). Data were collected from 190 to 260 nm in 1 nm steps, with 12 scans at each wavelength. However, the results were inconclusive due to background interference from Tris and high NaCl, both of which absorb strongly at far-UV wavelengths, as reflected by the high tension voltage reading of the instrument [Kelly, SM, Jess, TJ and Price, NC (2005), *Biochimica et biophysica acta* 1751:119-139]. To maximize the signal-to-noise ratio and minimize protein aggregation, the buffer was switched from Tris to phosphate and the effect of sequentially decreasing NaCl concentrations was examined. Specifically, SERT-Nter was first concentrated to 10 mg/ml (1135 μ M), diluted to 0.22 mg/ml (25 μ M), and then subjected to seven separate 15-minute analytical gel filtration runs (monitoring tryptophan fluorescence) on a Superdex 200 5/150 GL column (GE Healthcare) in 20 mM phosphate, pH 7.4, containing varying concentrations of NaCl: 0, 5, 10, 20, 50, 100, and 200 mM. SEC traces indicated that 20 mM was the lowest NaCl concentration at which SERT-Nter would not aggregate (c). Thus, final CD experiments on SERT-Nter were conducted in 20 mM phosphate, pH 7.4, and 20 mM NaCl. To ensure that the high tension voltage fell within the acceptable range of the Chirascan instrument (greater than 230V and less than 1000V), CD spectra were collected at four different SERT-Nter concentrations (25.0, 12.5, 6.3, and 3.1 μ M).

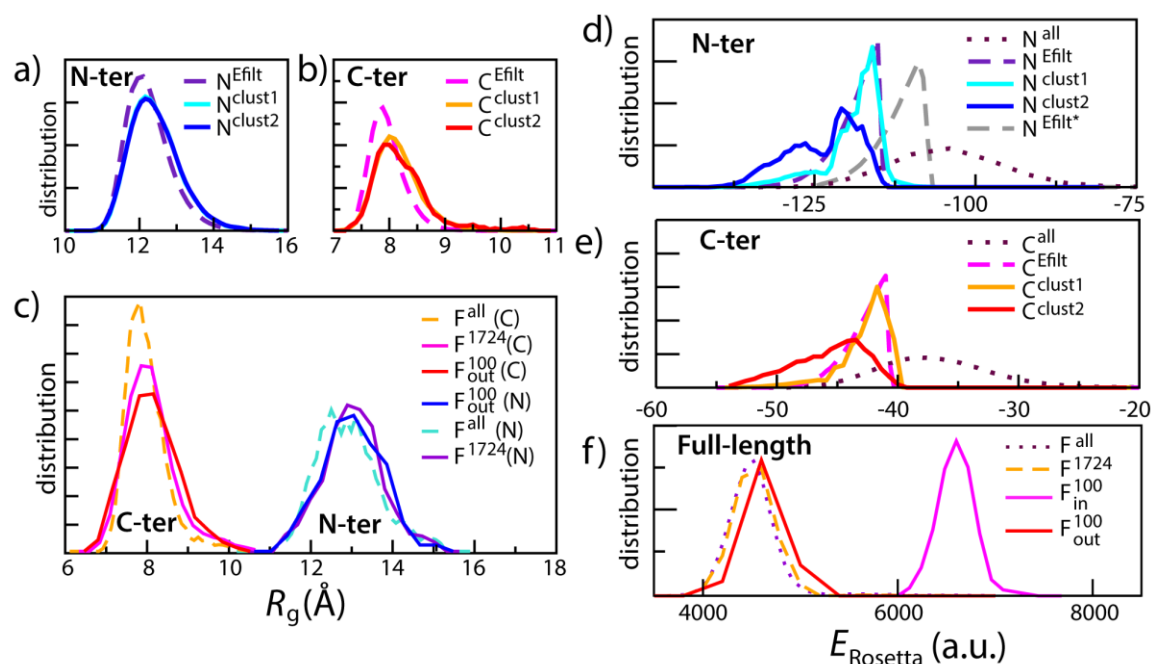


Figure S4. Assessment of the modeling protocol for terminal domain models of SERT. (a-c) Distribution of the radius of gyration (R_g) for: a) the N-terminal domain alone; b) the C-terminal domain alone and; c) the terminal domains in the context of the full-length protein. R_g was calculated for the backbone atoms of the N- and C-terminal domains. (a, b) The sets of models considered for the independent N- and C-terminal domains are: N^{Efilt} (purple dashed line), N^{clust1} (cyan), N^{clust2} (dark blue), C^{Efilt} (magenta dashed line), C^{clust1} (orange) and C^{clust2} (red). (c) The sets of full-length models are: $F^{\text{all}}(\text{N})$ and $F^{\text{all}}(\text{C})$ in cyan and orange dashed lines, respectively; $F^{\text{Efilt}}(\text{N})$ and $F^{\text{Efilt}}(\text{C})$, in purple and magenta, respectively; $F^{\text{out}100}(\text{N})$ and $F^{\text{out}100}(\text{C})$, in blue and red, respectively. (d-f) Distribution of Rosetta score (E_{Rosetta}) values for different sets of SERT models containing d) the N-terminal domain, e) the C-terminal domain and f) the full-length protein. (d, e) Data is shown for the domains in the following sets: N^{all} and C^{all} (brown dotted lines), N^{Efilt} (purple dashed line) and C^{Efilt} (magenta dashed line), N^{clust1} (cyan) and C^{clust1} (orange), N^{clust2} (blue) and C^{clust2} (red). $N^{\text{Efilt*}}$ (gray dashed line) is a 'decoy' set of N-terminal domains generated using a secondary structure prediction that is primarily coiled and only 2 positions are structured (see Figure 1a, SSP-full-SERT). (f) Distributions are shown for full-length complexes in the sets: F^{all} (purple dotted line), F^{1724} (orange dashed line), $F^{\text{out}100}$ (red) and $F^{\text{in}100}$ (magenta).

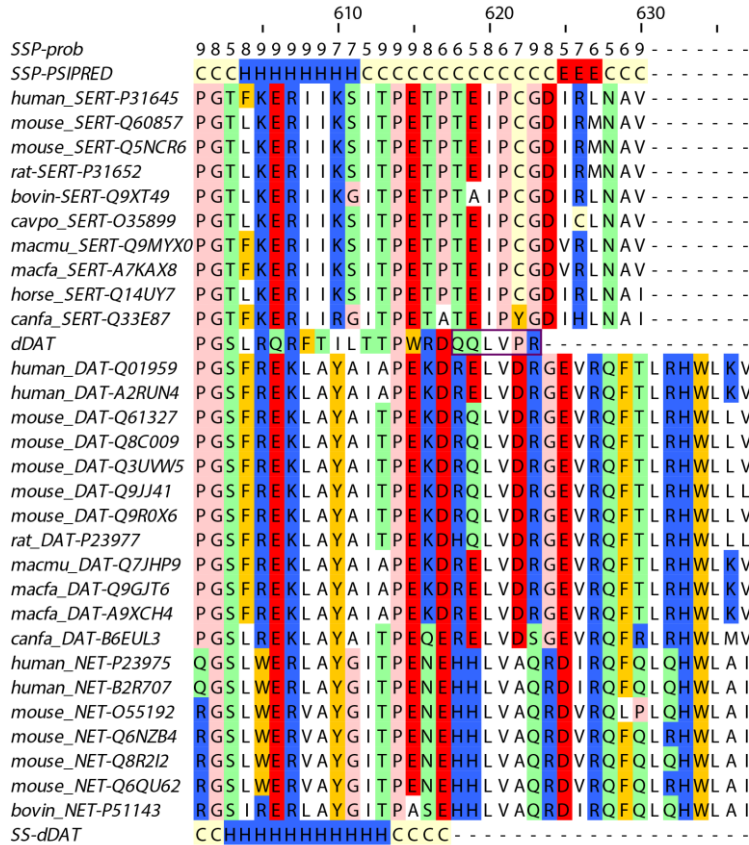


Figure S5. Helical elements in the C-terminal domains of SERT and DAT. A multiple-sequence alignment, of C-terminal domains of SERT and DAT orthologs with 95% coverage of human SERT or human DAT, respectively, and aligned according to [Sucic, S, El-Kasaby, A, Kudlacek, O, Sarker, S, Sitte, HH, Marin, P and Freissmuth, M (2011) *J Biol Chem*, 286:16482-16490] are compared with the secondary structure predictions (SSP-PSIPRED) for SERT and secondary structure annotations for *Drosophila melanogaster* dopamine transporter (SS-dDAT; last line). The region of the dDAT structure that is not resolved in the structure (PDB identifier 4M48) is outlined with a box. Sequence numbering corresponds to human SERT.

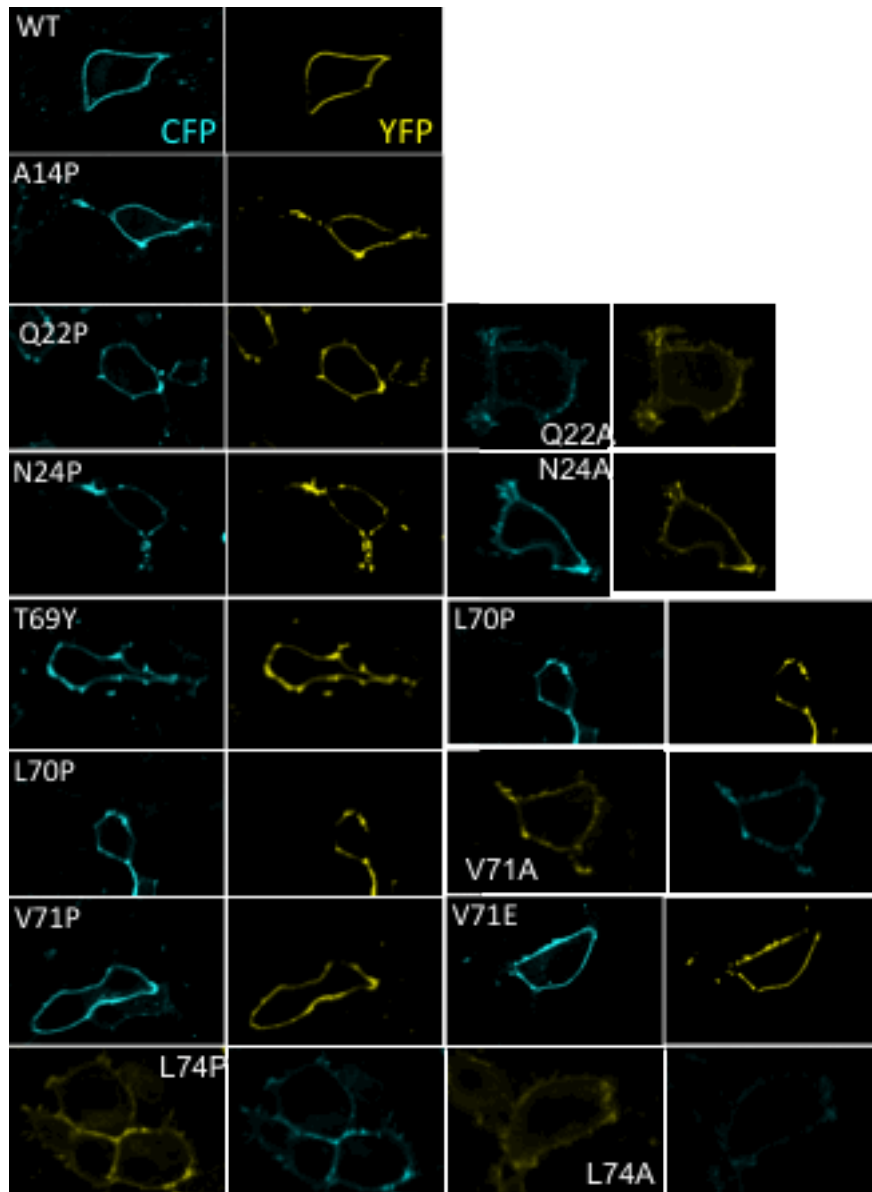


Figure S6. *Visualization of surface expression.* Confocal images demonstrating the surface expression of C-SERT-Y wild type and the indicated mutants in transiently-transfected HEK-293 cells; the abbreviation on the left image of each pair denotes the amino acids before/after mutation in the single letter code and its position in the SERT amino terminus. The left panel in each pair displays the CFP signal and the right panel shows the YFP signal for C-SERT-Y.

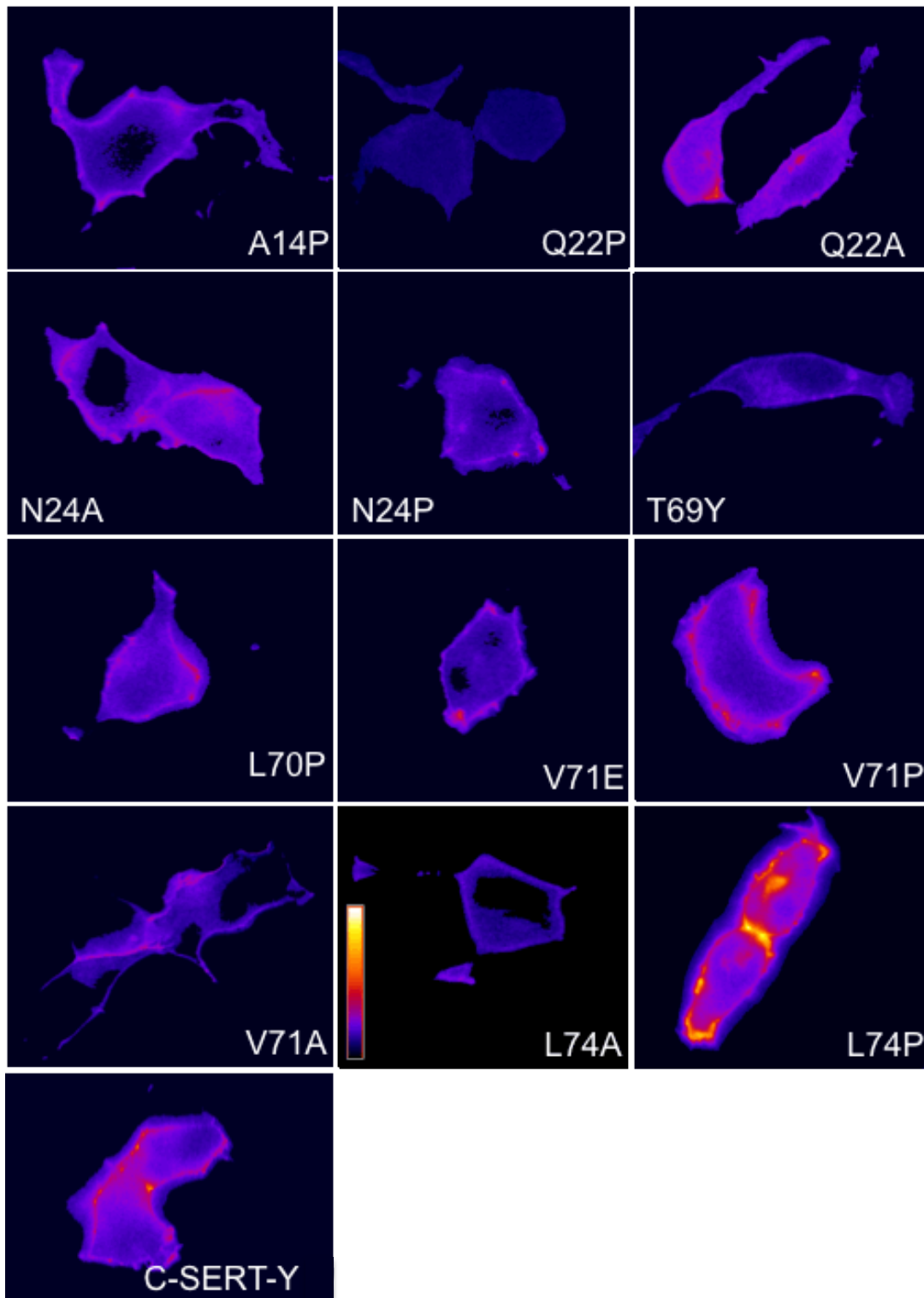


Figure S7. FRET images of C-SERT-Y and mutants thereof. FRET imaging and pixel-by-pixel analysis of the resulting images was performed in transiently transfected HEK293 cells as described in Experimental Procedures. The spatial distribution of the FRET signal in cells expressing the C-SERT-Y wild type and mutants is shown in representative images. The key displays the intensity of the arbitrary units.

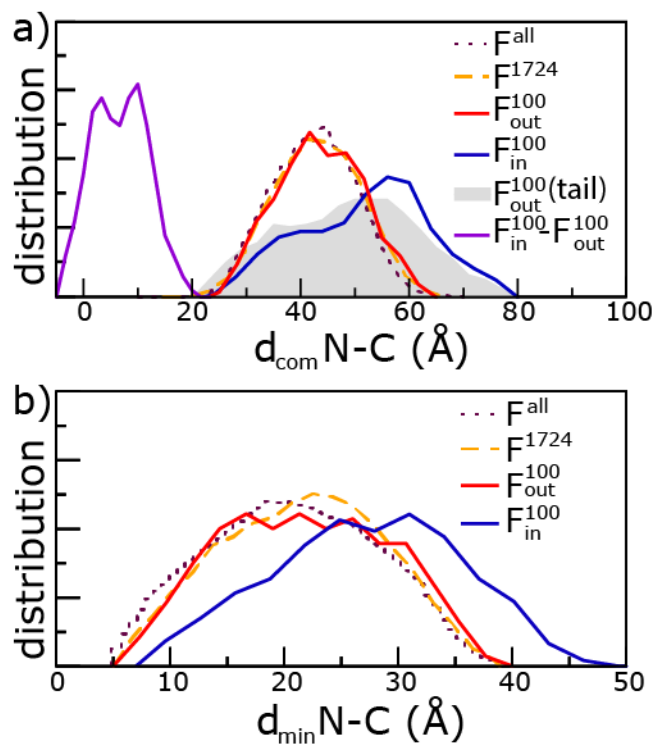


Figure S8. Distances between terminal domains in SERT full-length models. a) Distances between C α -atom centers of mass of the N- and C-terminal domains per model are plotted for the sets: F^{all} (purple dotted lines), F^{1724} (orange dashed lines), F_{out}^{100} (red), F_{in}^{100} (blue) as well as for the distance difference for each pair of terminal domains in inward- versus outward-open states (purple). Distance between centers of mass of the last or first three residues (tails) are also plotted for F_{out}^{100} (grey). b) Minimum distances between C α atoms of any pair of residues from the N- and C-terminal domains are plotted for: F^{all} (brown dotted lines), F^{1724} (orange dashed lines), F_{out}^{100} (red) and F_{in}^{100} (blue).

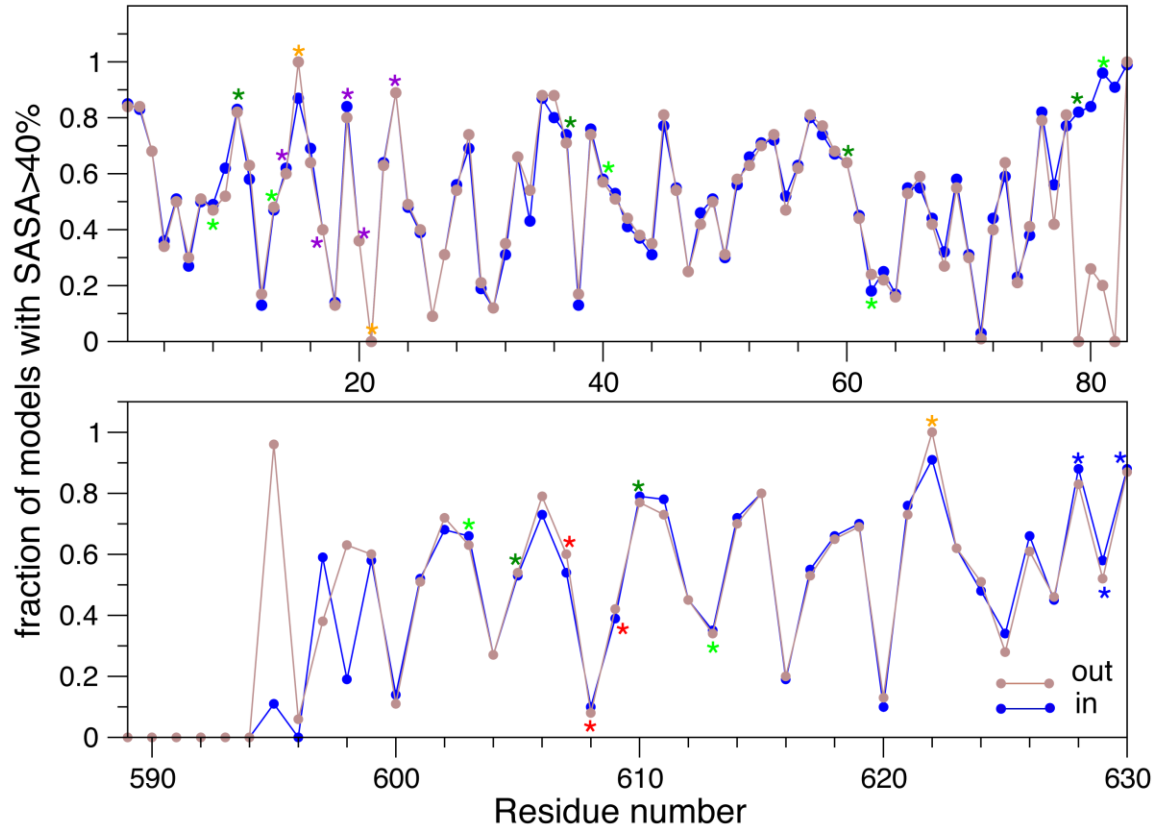


Figure S9. Solvent accessibility of residues in full-length models of SERT. (a) For every residue, the fraction of models out of 100 in which the percentage solvent accessible surface area (SASA) of that residue was >40% is plotted for the models in sets F_{out}^{100} (brown lines) and F_{in}^{100} (blue lines). Residues are marked with stars if they are proposed to: interact with syntaxin 1A (purple); be accessible to cysteine-modifying reagent (orange); be in the non-canonical PDZ-binding motif recognized by nNOS (dark blue); bind Sec24C (red); or be PKC phosphorylation sites (green). In each phosphorylation site, both the T or S residue (light green) that is predicted to be phosphorylated, and the K or R residue (dark green) required for phosphorylation are highlighted.

SUPPLEMENTARY TABLES

Table S1. *Primer sequences for C-hSERT-Y site-specific mutants*

A14P	ATTCTCAGAAGCAGCTATCACCGTGTGAAGATG
Q22P	GAAGATGGAGAAGATTGTCCGAAAACGGAGTTCTACAG
Q22A	GTGTGAAGATGGAGAAGATTGTGCGGAAAACGGAGTTCTAC
N24A	TGTGAAGATGGAGAAGATTGTCAGGAAGCCGGAGTTCTACAGAA
N24P	TGTGAAGATGGAGAAGATTGTCAGGAACCCGGAGTTCTACAGAA
T69Y	CCCAGCGACCACCACCTATCTAGTGGCTGAGCTTC
L70P	GACCACCACCACCCAGTGGCTGAGCTTC
V71E	CACCACCACCCTAGAGGCTGAGCTTCATC
V71P	CGACCACCACCACCTACCGGCTGAGCTTCATC
L74A	CACCCTAGTGGCTGAGGCTCATCAAGGGGAACGG
L74P	CCCTAGTGGCTGAGCCTCATCAAGGGGAACG
K610A	CCAGGGACATTTAAAGAGCGTATTATTGCAAGTATTACCCCAGAAACAC
K610P	CCAGGGACATTTAAAGAGCGTATTATTCCAAGTATTACCCCAGAAACAC